# The malaria circumsporozoite protein has two functional domains, each with distinct roles as sporozoites journey from mosquito to mammalian host

Alida Coppi,[1] Ramya Natarajan,[1] Gabriele Pradel,[2] Brandy L. Bennett,[1] Eric R. James,[3] Mario A. Roggero,[4] Giampietro Corradin,[4] Cathrine Persson,[5] Rita Tewari,[6] and Photini Sinnis[1]

[1]Department of Medical Parasitology, New York University School of Medicine, New York, NY 10010
[2]Research Center for Infectious Diseases, University of Würzburg, 97080 Würzburg, Germany
[3]Sanaria Inc., Rockville, MD 20850
[4]Department of Biochemistry, University of Lausanne, 1066 Epalinges, Switzerland
[5]Department of Molecular Biology, Umea University, SE-901 87 Umea, Sweden
[6]Center for Genetics and Genomics, School of Biology, The University of Nottingham, Nottingham NG7 2UH, England, UK

***Plasmodium*** **sporozoites make a remarkable journey from the mosquito midgut to the mammalian liver. The sporozoite's major surface protein, circumsporozoite protein (CSP), is a multifunctional protein required for sporozoite development and likely mediates several steps of this journey. In this study, we show that CSP has two conformational states, an adhesive conformation in which the C-terminal cell-adhesive domain is exposed and a nonadhesive conformation in which the N terminus masks this domain. We demonstrate that the cell-adhesive domain functions in sporozoite development and hepatocyte invasion. Between these two events, the sporozoite must travel from the mosquito midgut to the mammalian liver, and N-terminal masking of the cell-adhesive domain maintains the sporozoite in a migratory state. In the mammalian host, proteolytic cleavage of CSP regulates the switch to an adhesive conformation, and the highly conserved region I plays a critical role in this process. If the CSP domain architecture is altered such that the cell-adhesive domain is constitutively exposed, the majority of sporozoites do not reach their target organs, and in the mammalian host, they initiate a blood stage infection directly from the inoculation site. These data provide structure–function information relevant to malaria vaccine development.**

CORRESPONDENCE
Photini Sinnis:
photini.sinnis@nyu.edu

Abbreviations used: CSP, circumsporozoite protein; EEF, exoerythrocytic form; HBM-VEC, human brain microvascular endothelial cell; HSPG, heparan sulfate proteoglycan; i.d., intradermal(ly); IFA, immunofluorescence assay; MDF, mouse dermal fibroblast; PFA, paraformaldehyde; PV, parasitophorous vacuole; qPCR, quantitative PCR; TLP, Trap-like protein; TSR, type I thrombospondin repeat; UTR, untranslated region.

Malaria is one of the most important infectious diseases worldwide, causing an estimated 500 million clinical cases and 1–3 million deaths annually (Greenwood et al., 2005). Sporozoites, the infective stage of the malaria parasite, develop in mosquitoes and are inoculated into the mammalian host, where they ultimately must go to the liver, invade hepatocytes, and develop into exoerythrocytic stages (exoerythrocytic forms [EEFs]). Although sporozoites and the EEFs into which they develop are not associated with clinical symptoms, this is a time when

parasite numbers in the host are low and their eradication can completely abrogate infection. Indeed, sterile protection has been achieved in experimental settings using high doses of irradiated sporozoites, making the preerythrocytic stages of *Plasmodium* a focus of the malaria vaccine effort (Hoffman et al., 2002). Subunit vaccines based on circumsporozoite protein (CSP), such as RTS,S, are at the center of this endeavor. To date, the development of a malaria vaccine has been empirically driven and has yielded

promising though modest results (Ballou, 2009). Thus, an understanding of the molecular interactions between sporozoites and their mosquito and mammalian hosts is urgently needed to design rational interventions for this devastating disease.

The sporozoite's journey begins on the midgut of the mosquito host and ends within hepatocytes of the mammalian host. Sporozoites develop in oocysts on the midgut wall and are released into the hemocoel, where they are carried by the hemolymph throughout the mosquito's body cavity, ultimately attaching to and entering salivary glands. As infected mosquitoes probe for blood, sporozoites are injected into the skin of the mammalian host and actively move by gliding motility within the dermis to contact and penetrate blood vessels to enter the blood circulation (Amino et al., 2006). Exit from the dermal inoculation site requires that sporozoites traverse cell barriers via breaching the plasma membrane of the host cell (Mota et al., 2001; Amino et al., 2008), which is a qualitatively different process from cell invasion. Once in the circulation, sporozoites arrest in the liver, cross the sinusoidal barrier, and productively invade hepatocytes within a vacuole. Here they develop into EEFs, which, when mature, release merozoites that initiate blood stage infection.

The CSP forms a dense coat on the parasite surface and has been hypothesized to mediate many of the initial interactions between the sporozoite and its two hosts (Ménard, 2000;

Sinnis and Nardin, 2002). The structure of CSP is highly conserved among *Plasmodium* species infecting rodents, primates, and humans (Fig. 1 A). CSPs are comprised of a central repeat region that is diverse across *Plasmodium* species, and flanking the repeats are two conserved domains: region I, a 5-aa sequence at the N terminus of the repeats, and a known cell-adhesive motif C-terminal to the repeats termed the type I thrombospondin repeat (TSR). Studies with recombinant CSP, peptides representing portions of CSP, and sporozoites expressing heterologous CSP suggest that this protein targets sporozoites to both mosquito salivary glands and the mammalian liver (Aley et al., 1986; Cerami et al., 1992; Frevert et al., 1993; Sinnis et al., 1994; Chatterjee et al., 1995; Sidjanski et al., 1997; Pinzon-Ortiz et al., 2001; Suarez et al., 2001; Pradel et al., 2002; Rathore et al., 2002; Tewari et al., 2002, 2005). However, the region of CSP responsible for this targeting is debated: whereas some studies found that sequences within the TSR bound with high affinity to hepatocytes (Cerami et al., 1992; Frevert et al., 1993; Sinnis et al., 1994; Chatterjee et al., 1995), others found no hepatocyte-binding activity within the TSR and, in contrast, demonstrated that sequences within the N terminus of CSP bound specifically to hepatocytes (Aley et al., 1986; Suarez et al., 2001; Rathore et al., 2002). It is possible that these conflicting data are the result of peptides and recombinant proteins that do not accurately reproduce the correct folding of native CSP on the sporozoite surface.

Our laboratory has recently shown that proteolytic processing of CSP by a parasite cysteine protease occurs during invasion of hepatocytes (Coppi et al., 2005). Processing occurs on the sporozoite surface, and we identified the sulfation level of liver heparan sulfate proteoglycans (HSPGs) as the trigger of this event (Coppi et al., 2007). In this study, using antisera recognizing different regions of CSP and a series of *CSP* mutants, we define the cleavage site and elucidate the function of



**Figure 1.  *CSP* mutant parasites.** (A) Schematic diagram of CSP expressed in control and mutant parasites. The conserved region I and TSR are shown in blue, the species-specific repeats in yellow, and signal and anchor sequences in gray. Red lines show the length and location of the peptides used to make polyclonal antisera to the N- and C-terminal portions of CSP (α-N and α-C sera, respectively). (B) Western blot analysis of mutant salivary gland sporozoite lysates. The blot was cut in half, and the top was probed with polyclonal antiserum specific for TRAP as a loading control, and the bottom was probed with mAb 3D11 specific for the CSP repeat region. Molecular mass is indicated in kilodaltons. (C) Phase-contrast and fluorescence images of unpermeabilized mutant salivary gland sporozoites stained with mAb 3D11. Bar, 10 µm. Western blots and IFAs were repeated twice with similar results.

CSP processing. Our study demonstrates that CSP has a two-domain structure, with each domain having distinct functions as sporozoites migrate from mosquito to mammalian host. These functional experiments should inform the design of future CSP-based vaccines.

## RESULTS
### Region I contains the CSP cleavage site

Previous antibody mapping experiments as well as cleavage assays with sporozoites expressing a hybrid CSP indicated that proteolytic processing of CSP may occur within the highly conserved region I (Coppi et al., 2005). To test this hypothesis, we generated mutant sporozoites expressing CSP in which region I was deleted for comparison with a control parasite line expressing WT CSP (ΔRI and RCon sporozoites, respectively; Fig. 1 A and Fig. S1). The DNA constructs, $CSP^{\Delta RI}$ and $CSP^{RCon}$,

were separately introduced into the *Plasmodium berghei* ANKA genome through double homologous recombination, thus replacing the WT locus (Fig. S1). Recombinant parasites were selected with pyrimethamine and cloned by limiting dilution in mice, and correct integration of constructs was verified by PCR, Southern blotting (Fig. S1), and DNA sequencing (not depicted). Control parasites (RCon) were identical to WT *P. berghei* ANKA parasites in all aspects (unpublished data) and were used throughout this study for comparison with mutant lines.

Mutant ΔRI sporozoites expressed normal amounts of $CSP^{\Delta RI}$ as evaluated by Western blotting (Fig. 1 B). Furthermore, indirect immunofluorescence assays (IFAs) demonstrated that it was exported in normal amounts to the sporozoite surface (Fig. 1 C). To determine whether $CSP^{\Delta RI}$ was processed, we performed pulse-chase metabolic labeling experiments with sporozoites. Similar to WT CSP, the half-life
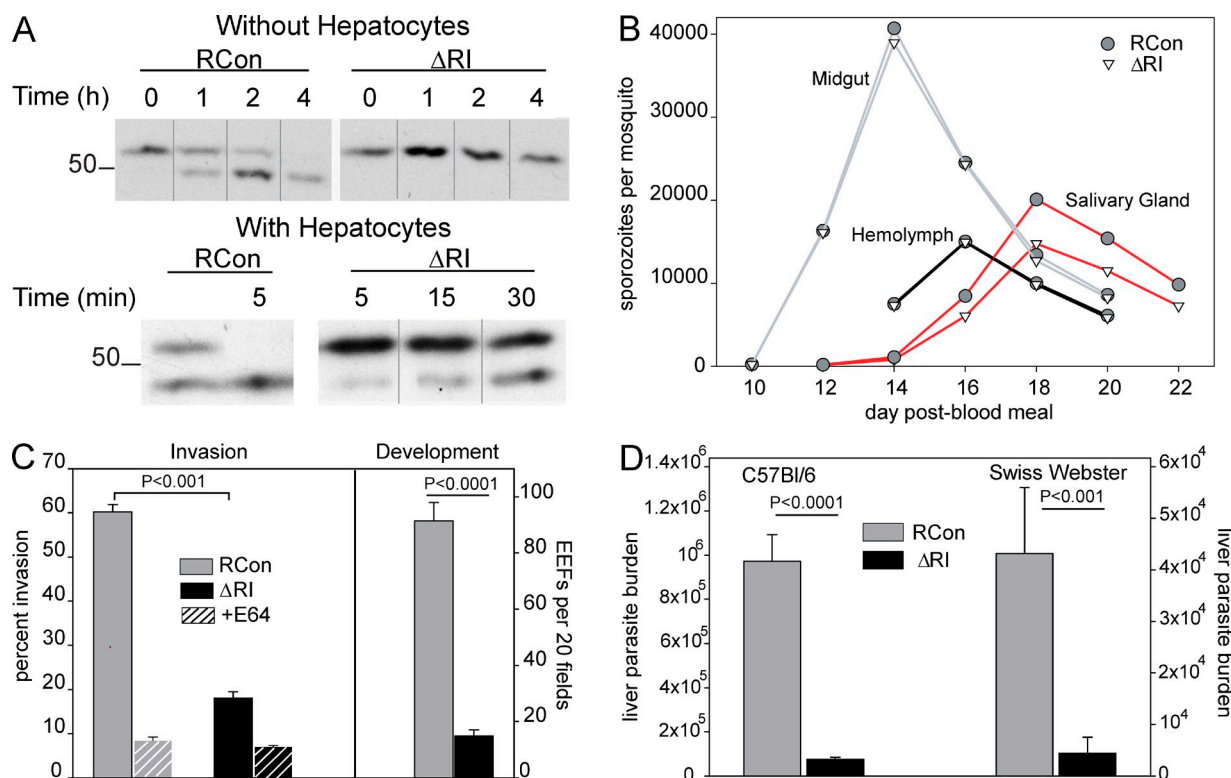


**Figure 2. Phenotype of ΔRI parasites.** (A) CSP processing in the absence and presence of hepatocytes. RCon and ΔRI salivary gland sporozoites were metabolically labeled with [35S]Cys/Met and kept on ice (time = 0) or chased for the indicated times after which they were lysed, and CSP was immunoprecipitated and analyzed by SDS-PAGE and autoradiography. For experiments with hepatocytes, labeled sporozoites were chased for 1 h in the absence of cells to give time for labeled CSP to be exported to the parasite surface (first lane for RCon and not depicted for ΔRI) and then added to Hepa1-6 cells for the indicated times, after which samples were processed as outlined above. Thin gray lines between lanes indicate that lanes were not contiguous on the scanned image of the autoradiograph. This experiment was performed three times, and a representative experiment is shown. Molecular mass is indicated in kilodaltons. (B) Sporozoite numbers in the mosquito host. Mosquitoes infected with RCon or ΔRI were dissected on the indicated days after blood meal, and the number of sporozoites associated with mosquito midguts, hemolymph, or salivary glands was determined. 20 mosquitoes were dissected per time point, and shown is the mean number per mosquito. This was repeated with three independent batches of infected mosquitoes, and a representative experiment is shown. (C) Infectivity in vitro. RCon or ΔRI sporozoites were added to Hepa1-6 cells and either fixed for an invasion assay (left) or grown for an additional 2 d before fixing and staining for EEFs (right). For invasion assays, parallel wells were seeded with sporozoites preincubated with E-64d (hatched bars) to determine the percentage of intracellular sporozoites that were in the process of cell traversal. 50 fields per well were counted, and shown are the means ± SD of triplicate wells. Each experiment was repeated three times with similar results. (D) Infectivity in vivo. C57BL/6 and Swiss Webster mice were injected i.v. with 10⁴ RCon or ΔRI sporozoites, and 40 h later, mice were sacrificed, total liver RNA was extracted, and liver parasite burden was determined by RT-qPCR. There are five mice per group, and shown are the means ± SD. Each experiment was performed three times with similar results.

of full–length CSP$^{RCon}$ was 1–2 h (Fig. 2 A, top; Coppi et al., 2005). In contrast, proteolytic processing of CSP$^{\Delta RI}$ was not detectable.

CSP processing occurs after the protein has been exported to the sporozoite surface and is a significantly more rapid process in the presence of hepatocytes, suggesting that contact with target cells triggers secretion or activation of the responsible protease (Coppi et al., 2005, 2007). To test the effect of cell contact on the kinetics of CSP$^{\Delta RI}$ cleavage, metabolically labeled RCon and $\Delta$RI sporozoites were chased for 1 h in the absence of cells, so that labeled CSP had time to be exported to the sporozoite surface, and then incubated with hepatocytes for different time periods. Cleavage of CSP$^{RCon}$ went to completion within 5 min of hepatocyte contact, whereas only 30% of labeled CSP$^{\Delta RI}$ was processed after 30 min (Fig. 2 A, bottom). These data demonstrate that CSP processing is significantly impaired in the absence of region I.

### CSP cleavage is not required in the mosquito host

To determine whether CSP cleavage has a biologically important function in the mosquito host, RCon or $\Delta$RI sporozoites were counted in oocysts, hemolymph, and salivary glands at different time points after blood meal. Deletion of region I had no effect on oocyst number, sporozoite development in oocysts, or sporozoite egress from oocysts (Fig. 2 B, Fig. S2, and Table S1). However, $\Delta$RI parasites consistently invaded salivary glands with a 10–15% lower efficiency compared with controls (Fig. 2 B and Table S1). To verify that $\Delta$RI salivary gland sporozoites had entered the salivary glands, we counted the number of salivary gland sporozoites after trypsinization, which removes sporozoites that have not invaded the glands, and found no difference in the ratio of external to internal sporozoites in $\Delta$RI-infected mosquitoes compared with controls (Table S2). Overall, these data indicate that CSP processing does not play a significant role in the mosquito host.

### CSP cleavage functions specifically during hepatocyte invasion

We next investigated whether CSP processing plays a role in the mammalian host. First, we compared the ability of RCon and $\Delta$RI sporozoites to invade and develop in Hepa1-6 cells, a hepatoma cell line which is permissive for infection by rodent malaria parasites. Although there was no difference in their ability to attach to cells (not depicted), $\Delta$RI sporozoites were significantly impaired in their ability to invade (Fig. 2 C). Because reliable markers for the early parasitophorous vacuole (PV) are lacking, it is difficult to distinguish intracellular sporozoites that have productively invaded from those that are in the process of migrating through. To address this, we performed invasion assays in the presence of E-64, which inhibits CSP processing and is known to greatly hinder invasion but not cell traversal (Coppi et al., 2005, 2007) and therefore allows us to estimate the proportion of intracellular sporozoites that are in the process of cell traversal. This can then be subtracted from the total proportion of intracellular

parasites to determine the fraction that have productively invaded. As shown in Fig. 2 C, $\Delta$RI sporozoites have an approximately fivefold reduction in their productive–invasive capacity in vitro. We also performed development assays and found that the defect in $\Delta$RI EEF development paralleled the defect in invasion (Fig. 2 C). However, the EEFs that did form were of normal size and morphology (Fig. S3), suggesting that CSP cleavage is required specifically for productive invasion and not for downstream processes.

We then tested the infectivity of $\Delta$RI sporozoites in vivo using C57BL/6 and Swiss Webster mice. When equal numbers of sporozoites were injected into mice i.v. and parasite liver load was determined 40 h later by RT–quantitative PCR (qPCR), infectivity of $\Delta$RI sporozoites was decreased 15-fold in C57BL/6 mice and 10-fold in Swiss Webster mice compared with controls (Fig. 2 D).

Because mosquitoes inject sporozoites into the dermis (Sidjanski and Vanderberg, 1997), we also analyzed the infectivity of $\Delta$RI sporozoites after intradermal (i.d.) inoculation. We monitored for the appearance of blood stage parasites (prepatent period). A 1-d delay in patency indicates a 90% decrease in the infective inoculum (Gantt et al., 1998). As shown in Table I, the route of inoculation did not significantly alter $\Delta$RI sporozoite infectivity, suggesting that processing of CSP is not required for sporozoite exit from the dermis.

Because cell traversal activity and gliding motility are required for dermal exit (Amino et al., 2006, 2008; Coppi et al., 2007), the similar infectivity of $\Delta$RI sporozoites after i.v. and i.d. inoculation suggests that they do not have deficits in motility or cell traversal. When tested in motility and migration assays in vitro, we found that this was the indeed the case (Fig. S4). In fact, $\Delta$RI sporozoites had enhanced cell traversal activity, a result which is consistent with the previous demonstration that inhibitors of invasion enhance cell traversal, suggesting that if sporozoites do not invade, they continue to migrate (Coppi et al., 2007).

Overall, these data suggest that the cleavage site lies within the highly conserved 5-aa sequence called region I and demonstrate that region I is required for rapid and complete processing of CSP. The small amount of cleavage observed in $\Delta$RI sporozoites may result from inefficient cleaving of an alternate site; however, limitations in the amount of material we can obtain for analysis preclude our being able to verify this hypothesis. Importantly, the phenotype of $\Delta$RI sporozoites definitively establishes the link between CSP cleavage and hepatocyte invasion and demonstrates that efficient cleavage requires region I.

### CSP changes conformation twice as sporozoites travel from mosquito midgut to mammalian liver

The precise function of proteolytic cleavage of CSP in the invasion process was not addressed by the $\Delta$RI mutant; therefore, we embarked on additional experiments to elucidate its role in this process. Because previous work indicated that the entire N-terminal third of CSP is removed after cleavage (Coppi et al., 2005), we investigated whether conformational

**Table I.** Infectivity of CSP mutant sporozoites as determined by prepatent period

| Experiment and mouse strain | Parasite line | Route of inoculation | Number of sporozoites injected | Number of mice positive/number of mice injected | Prepatent period |
|---|---|---|---|---|---|
| | | | | | *d* |
| **Experiment 1** | | | | | |
| Swiss Webster | RCon | i.v. | 5,000 | 5/5 | 3.0 |
| | RCon | i.d. | 5,000 | 5/5 | 3.0 |
| | ΔRI | i.v. | 5,000 | 5/5 | 5.0 |
| | ΔRI | i.d. | 5,000 | 5/5 | 5.0 |
| **Experiment 2** | | | | | |
| C57BL/6 | RCon | i.d. | 1,000 | 5/5 | 4.2 |
| | RCon | i.d. | 10,000 | 5/5 | 3.0 |
| | ΔNfull | i.d. | 1,000 | 0/5 | NA |
| | ΔNfull | i.d. | 10,000 | 5/5 | 13.8 |
| | ΔNfull | i.d. | 100,000 | 5/5 | 11.4 |
| **Experiment 3** | | | | | |
| Swiss Webster | RCon | i.d. | 1,000 | 5/5 | 4.6 |
| | RCon | i.d. | 10,000 | 5/5 | 3.0 |
| | ΔNfull | i.d. | 1,000 | 0/5 | NA |
| | ΔNfull | i.d. | 10,000 | 5/5 | 14.4 |
| | ΔNfull | i.d. | 100,000 | 5/5 | 12.0 |
| **Experiment 4** | | | | | |
| Swiss Webster | RCon | i.v. | 100 | 2/3 | 5.5 |
| | RCon | i.v. | 1,000 | 3/3 | 3.7 |
| | ΔNfull | i.v. | 100 | 3/3 | 3.0 |
| | ΔNfull | i.v. | 1,000 | 3/3 | 3.0 |

NA, not applicable.

changes in CSP were associated with cleavage. To test this, we performed IFAs on RCon sporozoites using polyclonal antisera directed against the N or C terminus of CSP. These antisera were generated using the long peptides shown in Fig. 1 A, and their fine specificity is presented in Fig. S5 and a previous publication (Coppi et al., 2005).

We tested the reactivity of surface CSP on different sporozoite populations, i.e., oocyst, hemolymph, and salivary gland. Interestingly, antisera specific for the C terminus bound to oocyst sporozoites but did not recognize hemolymph or salivary gland sporozoites, whereas antisera specific for the N terminus of CSP recognized hemolymph and salivary gland sporozoites but not oocyst sporozoites (RCon in Fig. 3 A). In these experiments, sporozoites were fixed with paraformaldehyde (PFA) and not permeabilized so that the conformation of surface CSP could be ascertained. These experiments were corroborated by experiments on live sporozoites stained at 4°C (unpublished data). We then tested the reactivity of salivary gland sporozoites after their addition to hepatocytes because CSP cleavage occurs upon contact with hepatocytes (Coppi et al., 2007). In the presence of hepatocytes, the majority of RCon sporozoites lost their reactivity to the N-terminal antiserum and gained reactivity to the C-terminal antiserum, suggesting that cleavage functions to unmask the

TSR (Fig. 3, B and C). The direct role of CSP cleavage in this event is demonstrated by the finding that ΔRI sporozoites retained reactivity to the N-terminal antiserum (Fig. 3 B and Fig. S6) and did not gain reactivity to C-terminal antiserum even after incubation with hepatocytes (Fig. 3 B). However, after prolonged contact with cells, a small proportion of ΔRI sporozoites were recognized by the C-terminal antiserum, which is consistent with our previous findings that CSP$^{ΔRI}$ is cleaved slowly and inefficiently (Figs. 2 A and 3, B and C).

Together, these data indicate that the cell-adhesive TSR of CSP is exposed twice during the sporozoite's life: during their development in the oocyst and after reaching their final destination, the hepatocyte. The phenotype of the ΔRI mutant indicates that proteolytic processing of CSP is required for TSR exposure in the mammalian host, i.e., during hepatocyte invasion, but not for its exposure during sporozoite development in the mosquito host.

### Mutants expressing cleaved CSP develop more sporozoites that are unable to target salivary glands

To further investigate the function of proteolytic processing of CSP, we generated a mutant parasite line in which the N-terminal third of the protein was deleted so that mutant sporozoites expressed only cleaved CSP on their surface

(ΔNfull sporozoites; Fig. 1 A and Fig. S1). This mutant was generated by replacement of the endogenous *CSP* locus with the *CSP*^ΔNfull allele and verified as previously outlined (Fig. S1). Protein expression and surface localization of CSP^ΔNfull were similar to WT CSP (Fig. 1, B and C). However, in contrast to WT sporozoites, this mutant expresses CSP in which the TSR is constitutively exposed (Fig. 3 A).

We first investigated the phenotype of the ΔNfull mutant in the mosquito, enumerating oocyst, hemolymph, and salivary gland sporozoites at the indicated time points after an infective blood meal. Interestingly, the ΔNfull mutant produced between 50 and 100% more sporozoites in oocysts compared with control lines (Fig. 4 A and Table S1). However, despite the high number of developing sporozoites, this
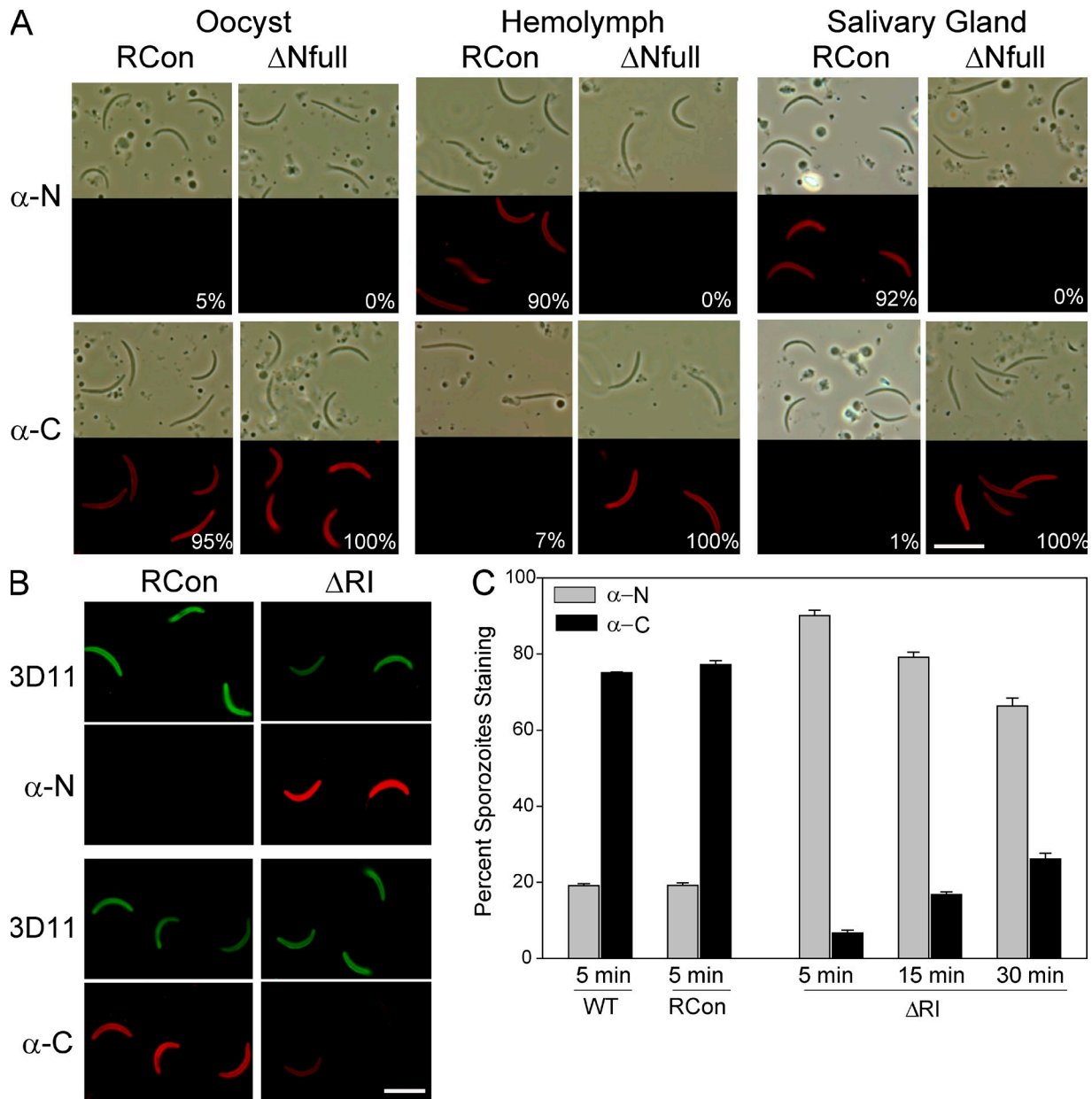


**Figure 3.  Exposure of the C–terminal TSR is a controlled process.** (A) Phase-contrast and fluorescence images of oocyst, hemolymph, and salivary gland sporozoites from RCon- and ΔNfull-infected mosquitoes stained with antiserum specific for the CSP N (α-N; top) or C terminus (α-C; bottom). The percentage of 200 sporozoites staining with each respective antiserum is shown. (B) Exposure of the C terminus on RCon and ΔRI sporozoites after contact with hepatocytes. Shown are fluorescence images of RCon and ΔRI salivary gland sporozoites 5 min after addition to Hepa1-6 cells stained with mAb 3D11, which stains all sporozoites (green), and α-N or α-C sera (red). (C) Graph showing the percentage of WT, RCon, or ΔRI salivary gland sporozoites staining with α-N or α-C sera at the indicated time points after their addition to Hepa1-6 cells. Total sporozoite number was determined by staining with mAb 3D11. Shown are the means of triplicate wells ± SD; 100 sporozoites per well were counted. All IFAs were repeated two to three times, and a representative experiment is shown. Bars, 10 μm.
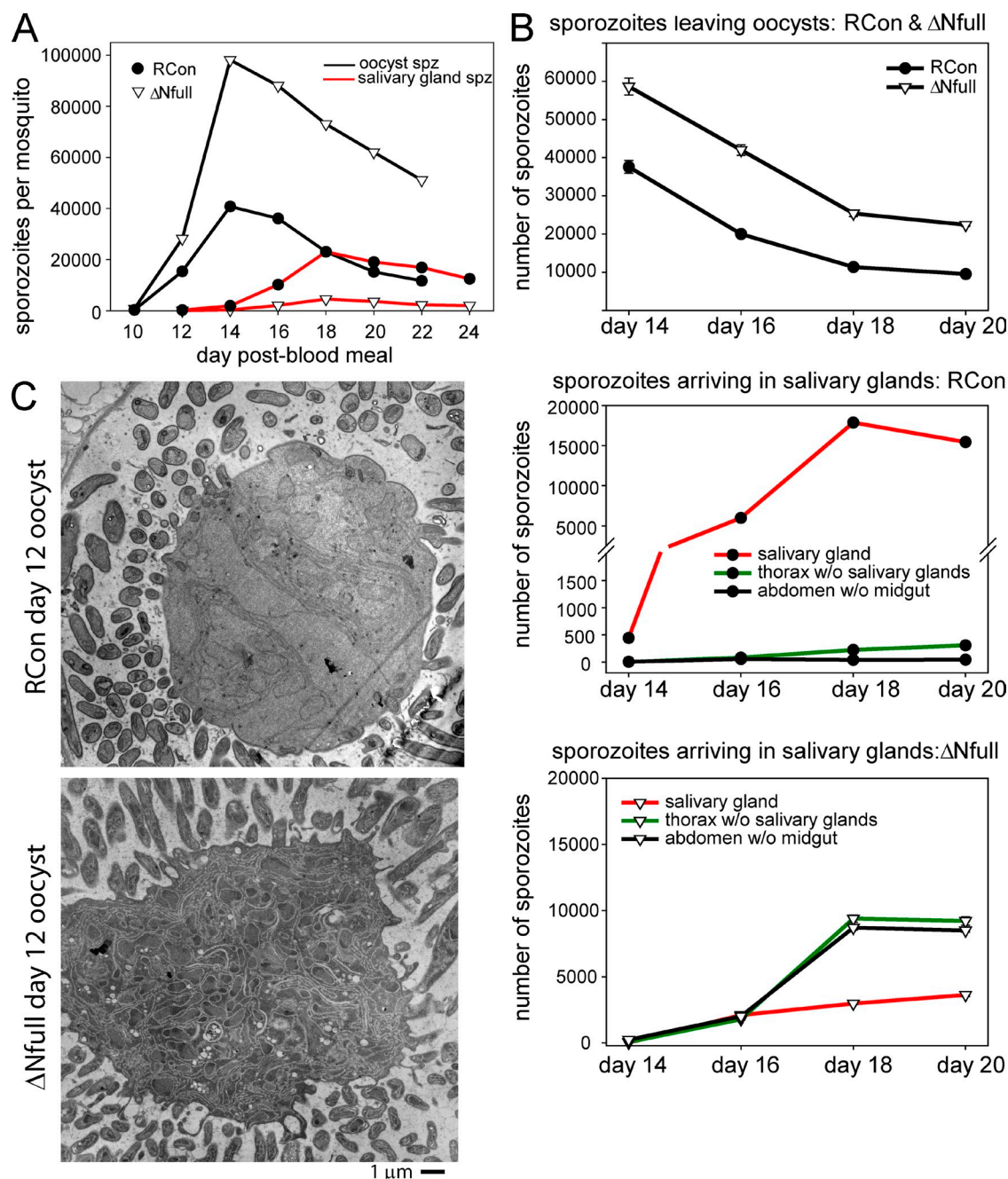
**Figure 4. Phenotype of ΔNfull sporozoites in the mosquito.** (A) Oocyst and salivary gland sporozoite numbers. Mosquitoes infected with RCon or ΔNfull parasites were dissected on the indicated days after blood meal, and the number of sporozoites (spz) associated with midguts or salivary glands was determined. 20 mosquitoes were dissected per time point, and shown is the mean number per mosquito. This was repeated with three independent batches of infected mosquitoes and a representative experiment is shown. (B) Distribution of ΔNfull sporozoites in the mosquito. Mosquitoes infected with RCon or ΔNfull parasites were dissected on the indicated days after blood meal, and midguts, salivary glands, thoraces without salivary glands, and abdomens without midguts were obtained, and the total number of sporozoites associated with each organ was determined by RT-qPCR. Organs from 20 mosquitoes were obtained per time point, and shown is the mean number of RCon and ΔNfull sporozoites associated with the mosquito midgut over time (top), the mean number of RCon sporozoites associated with salivary glands, the thorax, or abdomen over time (middle), and the mean number of ΔNfull sporozoites associated with salivary glands, thorax, or abdomen over time (bottom). The experiment was performed twice with similar results. (C) Transmission electron micrographs of oocysts from mosquitoes infected with RCon or ΔNfull parasites at day 12 after blood meal. Between 8 and 12 oocysts were observed per parasite line, and an average of two sections per oocyst was performed. Shown are representative images.

mutant consistently had 10-fold fewer salivary gland sporozoites compared with controls (Fig. 4 A and Table S1).

Increased numbers of sporozoites could have one of two causes: either the mutant produces more oocysts, or within each oocyst more sporozoites develop. Comparison of oocyst numbers in RCon- and ΔNfull-infected mosquitoes revealed no differences (Fig. S2), suggesting that within each ΔNfull oocyst, more sporozoites developed. Sporozoites develop in oocysts by schizogony, a replication process in which nuclear division precedes the formation of daughter cells (Sinden and Strong, 1978). The early oocyst contains one or more cytoplasmic islands called sporoblasts, and sporozoites bud from sporoblasts at sites where an inner membrane complex has been deposited along the plasmalemma. As the sporozoite buds, cytoplasmic components such as the nucleus, mitochondria, and other organelles are pulled into the forming sporozoite. Ultimately, the oocyst is full of sporozoites, and the sporoblast resembles a residual body. To examine this process in the ΔNfull mutant, we performed electron microscopy on oocysts from infected mosquito midguts. At early time points after infective blood meal, we saw no differences in the morphology between RCon and ΔNfull oocysts (Fig. S7 A). However, once sporozoite budding began, sporoblasts from ΔNfull mutant oocysts exhibited increased budding (Fig. 4 C and Fig. S7, A and B). These sporozoites showed normal morphology, having a canonical crescent shape and size with one nucleus per sporozoite (Fig. S7, B and C). Thus, the conformation of CSP in the ΔNfull mutant leads to enhanced budding and increased numbers of sporozoites developing in the oocyst.

Despite these increased numbers, there was a 10-fold reduction in the number of ΔNfull sporozoites that reached the salivary glands (Fig. 4 A and Table S1). To better understand this, we followed the distribution of ΔNfull and RCon sporozoites in the mosquito over time by RT-qPCR. Both RCon and ΔNfull sporozoites exited oocysts between days 14 and 20 after blood meal (Fig. 4 B, top). After their release from oocysts, RCon sporozoite numbers increased in salivary glands, and only small numbers of these sporozoites were found associated with other tissues (Fig. 4 B, middle). In contrast, after their release from oocysts, ΔNfull sporozoites were found throughout the mosquito and only in low numbers in salivary glands (Fig. 4 B, bottom). However, the ΔNfull sporozoites that did make it to the salivary glands were able to invade the glands in proportions similar to controls (Table S2). Overall, these data suggest that exposure of the cell-adhesive TSR on hemolymph ΔNfull sporozoites leads to their nonspecific adhesion throughout the mosquito, thus explaining why they do not reach the salivary glands in sufficient numbers.

### Mutants expressing cleaved CSP have enhanced infectivity

ΔNfull sporozoites that successfully reached the salivary glands could be used to investigate the role of the N terminus of CSP as well as the function of its removal in the mammalian host. In vitro, ΔNfull salivary gland sporozoites displayed a higher invasion efficiency compared with controls (Fig. 5 A). Because we could not use E–64 to distinguish between productively invaded versus migratory sporozoites as CSP$^{\Delta Nfull}$ is expressed as its cleaved form, we stained intracellular parasites with antisera to UIS-4, a marker for the PV (Tarun et al., 2007). UIS-4 staining indicated that the majority of ΔNfull mutants had productively invaded the cells (Fig. 5 A), and this was confirmed by the finding that they also produced more EEFs compared with
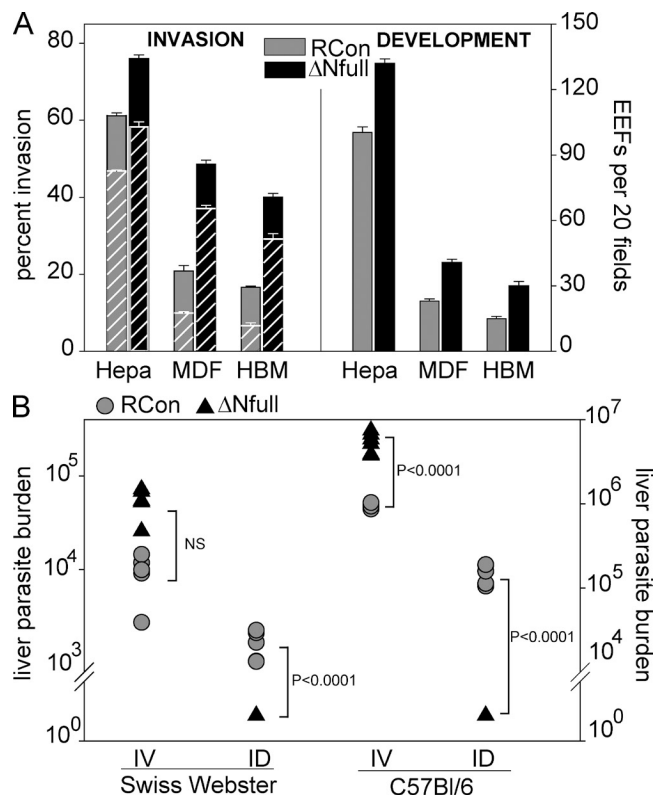


**Figure 5. Infectivity of ΔNfull sporozoites in the mammalian host.** (A) In vitro infectivity. RCon or ΔNfull sporozoites were added to Hepa1-6 (Hepa), MDFs, or HBMVEC (HBM) for 1 h (invasion), 6 h (PV formation), or 2 d (EEF development), fixed, and stained. Invasion was scored using a double staining assay that distinguishes intracellular from extracellular sporozoites, and shown is the percentage of total sporozoites that are intracellular (left). To determine whether sporozoites entered in a vacuole, replicate wells were fixed 6 h after infection and stained with mAb 3D11 and anti–UIS-4, a marker for the PV, and shown is the percentage of total sporozoites that are in a vacuole (left; hatched bars). In the right panel, the number of EEFs developing for each parasite line is shown. For each experiment, 50 fields per well were counted, and shown are the means ± SD of triplicate wells. The difference in invasion efficiency and EEF development between RCon and ΔNfull sporozoites in all cell lines was significant with p-values <0.01. Experiments were repeated three times with similar results. (B) In vivo infectivity. Mice were injected either i.v. or i.d. with 10⁴ RCon or ΔNfull sporozoites, and 40 h later, total liver RNA was extracted, and liver parasite burden was determined by RT-qPCR. There were five mice per group, and the liver parasite burden of each mouse is shown. The experiment was performed three times with similar results.

controls (Fig. 5 A). We also tested the infectivity of ΔNfull sporozoites for normally less permissive cell lines such as mouse dermal fibroblasts (MDFs) and an endothelial cell line (human brain microvascular endothelial cell [HBMVEC]) and found that ΔNfull sporozoites also have enhanced invasive capacity for these cell lines (Fig. 5 A). The enhanced infectivity of ΔNfull sporozoites suggests that these parasites are primed for invasion because CSP on their surface is already cleaved.

We next determined the infectivity of ΔNfull sporozoites in vivo. When injected i.v., the results paralleled the in vitro data in that these sporozoites had higher infectivity in both Swiss Webster and C57BL/6 mice (Fig. 5 B and Table I). However, in contrast to the enhanced infectivity observed after i.v. inoculation, we could not detect parasite signal in the liver after i.d. inoculation of ΔNfull sporozoites (Fig. 5 B). To further investigate the infectivity of ΔNfull sporozoites after i.d. inoculation, we injected sporozoites and then monitored for blood stage infection. The rationale for these experiments is that the RT-qPCR assay may not detect very low numbers of developing parasites in the liver, whereas a single infected hepatocyte will give rise to a detectable blood stage infection. As shown in Table I, i.d. inoculation of $10^3$ or $10^4$ RCon sporozoites resulted in a detectable blood stage infection by days 3–4 after inoculation. In contrast, i.d. inoculation of $10^3$ ΔNfull sporozoites never gave rise to a blood stage infection. However, when we inoculated higher numbers, $10^4$ and $10^5$ ΔNfull sporozoites, we observed blood stage infections with a 10-d delay compared with controls (Table I). In the next section, we outline experiments performed to investigate the large difference in infectivity of ΔNfull sporozoites after i.v. versus i.d. inoculation.

Previous studies have shown that in the mammalian host, inoculated sporozoites have two distinct states of being: they can be in a migratory mode, traversing cells with which they come into contact, or they can be in an invasive mode, which leads to cell entry in a vacuole and progression to the next life cycle stage (Mota et al., 2002; Coppi et al., 2007; Amino et al., 2008). We have previously found that sporozoites that are inhibited from invading remain in migration mode (Coppi et al., 2007). Thus, we would predict that sporozoites that are primed for invasion would migrate less. When we quantified the migratory activity of ΔNfull sporozoites, we indeed found that they were less migratory compared with controls, supporting the hypothesis that they have an invasive phenotype (Fig. S4).

## Mutants expressing cleaved CSP do not exit the dermis and initiate infection from this site

Because mosquitoes inoculate sporozoites i.d. (Sidjanski and Vanderberg, 1997; Medica and Sinnis, 2005; Amino et al., 2006), infectivity by this route of entry is critical for continuation of the parasite's life cycle. Our results indicate that by the i.d. route, ΔNfull sporozoites have a very low capacity to initiate malaria infection possibly because these sporozoites cannot exit the dermis. To test this, we measured sporozoite numbers at the injection site after i.d. inoculation by qPCR. As shown in Fig. 6 A,



A

C

| Time ear cut (h) | Number of Mice Positive | Prepatent period (days) |
|---|---|---|
| not cut | 10/10 | 13.7 |
| 22 | 0/5 | -- |
| 38 | 0/5 | -- |
| 40 | 0/5 | -- |
| 65 | 5/10 | 21.8 |
| 90 | 9/10 | 17.4 |
| 115 | 10/10 | 15.7 |

B

**Figure 6. ΔNfull sporozoites do not exit the dermis and can seed the blood directly from this location.** (A) Kinetics with which ΔNfull parasites disappear from the inoculation site. Swiss Webster mice were injected i.d. in the ear with 5,000 RCon or ΔNfull sporozoites, ears were removed at the indicated time points, and the number of sporozoites in each ear was quantified by qPCR. There are four mice per group, and shown are the means ± SD. The differences between RCon and ΔNfull sporozoite numbers remaining in the skin at 18–90 h were statistically significant with p-values <0.001, whereas differences in sporozoite numbers at earlier times points did not reach significance. The experiment was performed twice with similar results. (B) Expression of sporozoite- and EEF-specific genes at the inoculation site. Swiss Webster mice were injected with RCon (left) or ΔNfull (right) sporozoites i.d., ears were removed at the indicated time points, total RNA was extracted, and the expression of TLP and MSP-1 was quantified by RT-qPCR. There were four mice per group, and shown are the means ± SD. (C) Removal of the inoculation site between 22 and 40 h after sporozoite injection abrogates blood stage infection by ΔNfull sporozoites. $10^4$ ΔNfull sporozoites were inoculated i.d. into one ear, and the ear was either left intact or removed at the indicated time points. All mice were followed for 30 d for the appearance of blood stage parasites by Giemsa-stained blood smears. Shown are the combined results of two independent experiments.
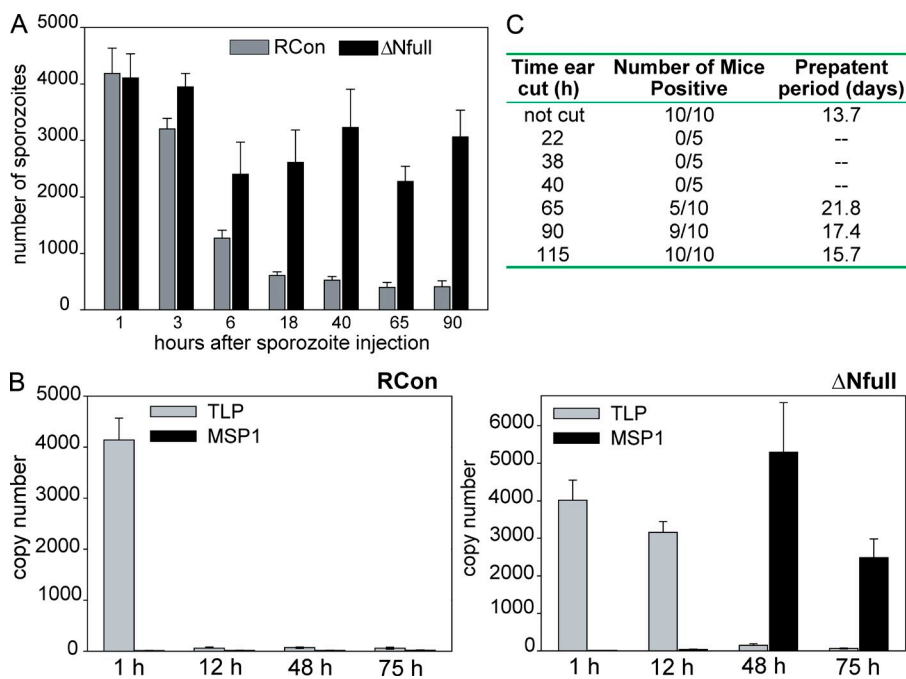
RCon sporozoites disappeared from the injection site with kinetics similar to what has been previously published for *Plasmodium yoelii* sporozoites (Yamauchi et al., 2007). In contrast, ΔNfull sporozoite numbers in the injection site decreased only marginally over time (Fig. 6 A), demonstrating that they do not efficiently exit the dermis. To determine whether they are developing in this location, we measured sporozoite- and EEF-specific transcripts in the dermal inoculation site over time. As shown in Fig. 6 B, Trap-like protein (TLP) transcripts, which are specific to the sporozoite stage (Moreira et al., 2008), were robustly detected after RCon or ΔNfull sporozoite inoculation into the dermis (Fig. 6 B). 12 h later, ΔNfull sporozoites remained in the skin, and TLP transcripts continued to be detected, whereas RCon sporozoites had exited the inoculation site (Figs. 6, A and B). Interestingly, at 48 h after ΔNfull sporozoite inoculation, we no longer detected TLP transcripts but observed robust expression of MSP-1 (merozoite surface protein 1) transcripts, which are associated with the development of merozoites in late stage EEFs (Fig. 6 B; Sinden et al., 1990).

These findings raised the possibility that blood stage infection after i.d. inoculation of ΔNfull sporozoites was caused by parasites that remained in the skin. To that end, we inoculated ΔNfull sporozoites into the ears of mice, removed the inoculation site at different time points, and monitored the mice for blood stage infection. Normal development of rodent malaria EEFs takes ∼46 h. Interestingly, none of the mice whose ears were removed at 22, 38, or 40 h after sporozoite inoculation became patent for blood stage parasites, whereas mice whose ears were removed at later time points developed blood stage infections (Fig. 6 C). These data suggest that ΔNfull parasites are seeding the blood directly from the inoculation site. Furthermore, the significantly prolonged prepatent periods observed suggest that this occurs with low efficiency, possibly because of the difficulty that merozoites of mature skin EEFs have in accessing the blood circulation. Although these data could also be explained by a few ΔNfull sporozoites that lingered at the

inoculation site for >40 h before leaving, if this were the case, we would expect to see blood stage infection with a 2–4-d delay rather than 10-d delay because once in the liver, ΔNfull sporozoites develop normally.

## Mutants expressing cleaved CSP gain susceptibility to antibodies targeting the TSR

The phenotype of ΔNfull sporozoites suggests that one function of masking the TSR is to maintain the sporozoites in a migratory state, enabling them to complete their journey to the liver. To test whether this has an additional role of protecting sporozoites from antibodies targeting an important functional domain, the TSR, we compared the infectivity of RCon and ΔNfull sporozoites in the presence of polyclonal antisera specific for the C terminus. As shown in Fig. 7, polyclonal antisera specific for the C terminus had no effect on RCon sporozoite infectivity in vitro or in vivo. In contrast, ΔNfull sporozoites were inhibited from invading Hepa1-6 cells in the presence of this antiserum, and their infectivity was significantly diminished in vivo when mice were preinjected with the antiserum. These data suggest that unmasking the C terminus at the moment of hepatocyte contact also functions to protect sporozoites from antibodies targeting the TSR.

## DISCUSSION

The data presented in this study provide a molecular basis for understanding how sporozoites travel from mosquito midgut to mammalian liver, a journey which must be completed to establish infection. Although a significant amount of previous work has demonstrated that CSP has critical roles in many steps of this journey (Ménard, 2000; Sinnis and Nardin, 2002), there has been no unifying hypothesis as to how one protein functions in so many disparate events. In this study, we show that CSP has two conformational states, an adhesive conformation in which the TSR is exposed and a nonadhesive conformation in which the TSR is masked by the N terminus. Furthermore, we show that each of these conformations is associated with distinct functional properties. The TSR-exposed conformation occurs at the
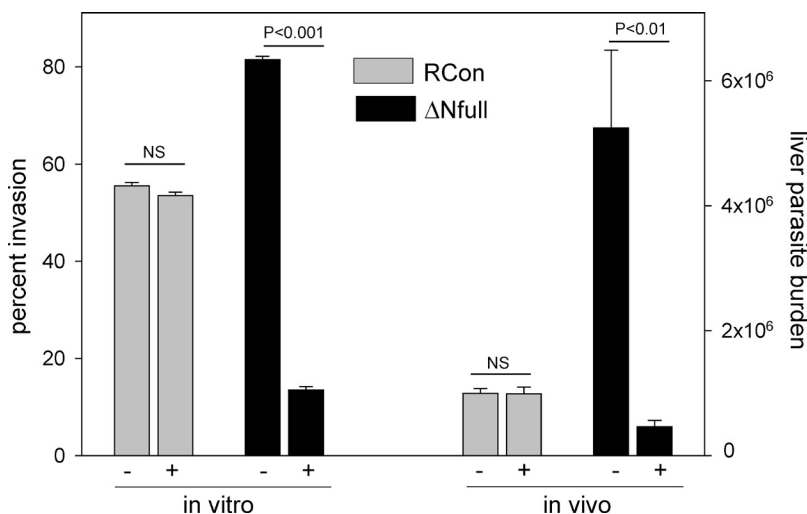


**Figure 7. Just–in–time exposure of the TSR protects sporozoites from antibody–mediated inhibition.** The effect of α-C serum on the infectivity of RCon and ΔNfull sporozoites was tested in vitro (left) and in vivo (right). In vitro, sporozoites were added to Hepa1-6 cells in the presence (+) or absence (−) of α-C serum for 1 h, cells were fixed and stained, and the percentage of intracellular sporozoites was determined. 50 fields per well were counted, and shown are the means ± SD of triplicate wells. In vivo, α-C serum (+) or buffer alone (−) was injected i.v. into C57BL/6 mice, and 5 min later, 10^4 RCon or ΔNfull sporozoites were inoculated i.v., and 40 h later, liver parasite burden was determined by RT-qPCR. There are five mice per group, and shown are the means ± SD. Each experiment was performed three times with similar results.

two ends of the sporozoite's life, during sporozoite development and hepatocyte invasion. Moreover, the phenotype of our CSP mutants suggests that the TSR functions during these two critical processes. Between these two spatially and temporally distinct events, the N terminus masks the TSR, a conformation which confers a migratory phenotype upon sporozoites. This is supported by our finding that sporozoite mutants in which the N terminus is deleted adhere throughout the mosquito hemocoel and cannot exit the mammalian dermis though they are fully infectious when inoculated i.v. In the mammalian host, proteolytic cleavage within region I is the link between the nonadhesive and adhesive conformation of CSP. A model summarizing these data is shown in Fig. 8.

This model changes the currently held view that the TSR targets sporozoites to the liver (Ménard, 2000; Sinnis and Nardin, 2002), a hypothesis which was based on studies with recombinant CSP demonstrating that the TSR binds specifically to hepatic HSPGs (Cerami et al., 1992; Frevert et al., 1993; Sinnis et al., 1996) and on the previously accepted notion that inoculated sporozoites rapidly target the liver (Cerami et al., 1994; Sinnis et al., 1996). Recent studies demonstrating that sporozoites are inoculated into the dermis (Sidjanski and Vanderberg, 1997) and exit this location in a slow trickle that extends for hours (Yamauchi et al., 2007) suggest that the old model may be in need of revision. Our demonstration that premature exposure of the TSR prevents sporozoites from reaching the liver when inoculated into the skin (as they are in natural infection) provides further support for this revision.

Our new model (Fig. 8) is in agreement with recent work demonstrating that sporozoites are in a migratory noninvasive state when inoculated into the skin and that they become activated for invasion after reaching the liver (Mota et al.,

2002; Coppi et al., 2007; Amino et al., 2008). Our data expand on this previous work and establish a link between the activation state of the sporozoite and the conformation of CSP. ΔRI sporozoites, which are significantly impaired in their ability to cleave CSP and so retain full-length CSP on their surface, are poorly infectious yet have enhanced migratory activity. In contrast, ΔNfull sporozoites, which express cleaved CSP on their surface, have enhanced infectivity and are less migratory. Furthermore, these data support the notion that the TSR is involved in the invasion process itself; however, its role in this process remains to be determined. Although the environmental signal or signals that trigger activation are the subject of debate, it is likely that the highly sulfated HSPGs of hepatocytes are involved in this process (Coppi et al., 2007). Importantly, the link between a cell's adhesiveness and its activation state is found in several other biological systems, including the immune system (Springer, 1990).

In the mammalian host, dermally inoculated ΔNfull mutants cannot exit the dermis but develop and initiate blood stage infection from the inoculation site. Previous studies have shown that a small proportion of WT rodent malaria sporozoites remain in the dermis and can develop into what appear to be mature EEFs (Gueirard et al., 2010; unpublished data). However, given the low numbers of these skin EEFs, it has been difficult to demonstrate that they can initiate a blood stage infection. In contrast, ΔNfull sporozoites express CSP in the adhesive, TSR–exposed conformation, which leads to a larger proportion of the inoculum remaining in the skin and confers upon these sporozoites an enhanced infectivity for normally less permissive cell types. Thus, these sporozoites may be a good tool to study skin stage EEFs in vivo. The very long prepatent periods observed after i.d. inoculation
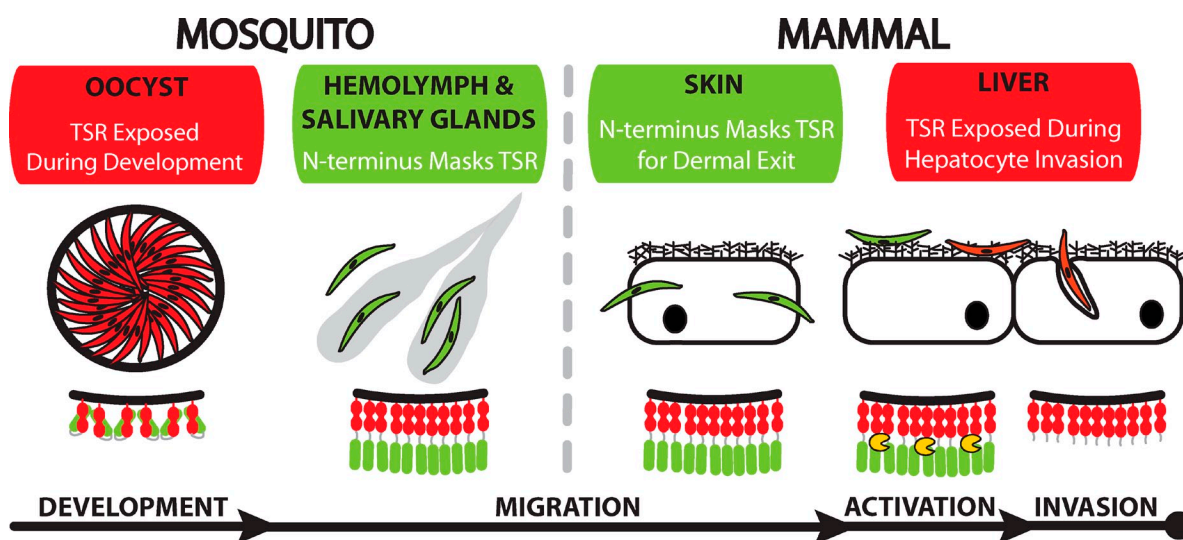


**Figure 8.   A model for the role of CSP in the sporozoite's journey.** Model showing the correlation between the conformation of CSP on sporozoites and their location/developmental stage in both mosquito and mammalian hosts. Below each heading is a picture of sporozoites in that location, in which green sporozoites have the N terminus exposed and red sporozoites have the C terminus exposed. Below each group of sporozoites is a schematic of CSP, in which green shows the N terminus, red shows the C terminus, gray shows the repeats, and in yellow is the protease that cleaves CSP.

of ΔNfull sporozoites is unusual as one sporozoite successfully infecting a hepatocyte can lead to a blood stage infection in 7–8 d. We hypothesize that this is because the skin lacks easy access to the blood circulation, making it difficult for merozoites to access their target, the erythrocyte. Thus, it is likely that only a very small number of the merozoites that develop in ΔNfull skin EEFs ultimately reach the blood, which in turn would necessitate several rounds of multiplication before sufficient parasite numbers accumulate such that they are detectable by blood smear.

Although our data suggest how the domain structure of CSP can confer multiple functions, several questions remain as to the precise roles played by both the TSR and the N-terminal domain. In the case of the TSR, our findings build upon previous studies demonstrating a critical role for CSP in sporozoite development (Ménard et al., 1997; Thathy et al., 2002). Specifically, our demonstration that the TSR of CSP is exposed in oocyst sporozoites and that ΔNfull oocysts exhibit significantly increased sporozoite budding suggests a role for this domain in the budding process. The TSR is found in >100 proteins, and studies of other TSR–containing proteins such as UNC-5 and F-Spondin show that this domain is involved in guiding cell migration in the developing nervous system (Adams and Tucker, 2000). Thus, it is possible that the TSR plays a role in guiding budding sporozoites into the oocyst vacuolar space, and further studies testing this hypothesis are underway. Although we demonstrate that the TSR of CSP is exposed on oocyst sporozoites, proteolytic cleavage is not required for TSR exposure in this location because sporozoite development is not affected in cleavage site mutants. Therefore, it is possible that a chaperone protein binds to CSP in oocysts to maintain the exposure of the TSR and then dissociates as sporozoites exit the oocyst, leading to a conformational change in CSP.

Our findings suggest that the N-terminal third of CSP forms a functional domain whose role is to mask the cell–adhesive TSR. However, the N terminus may also have adhesive properties of its own. This hypothesis is supported by previous studies demonstrating that the N terminus of CSP binds specifically to mosquito salivary glands (Sidjanski et al., 1997; Myung et al., 2004). Thus, the N terminus may both prevent nonspecific adhesion of sporozoites throughout the mosquito hemocoel and in some way aid sporozoites in targeting salivary glands. If this is the case, the interaction between the CSP N terminus and the salivary gland surface is likely to be a low affinity recognition event that is followed by high affinity interactions with other sporozoite ligands such as MAEBL and TRAP (Kariu et al., 2002; Saenz et al., 2008; Ghosh et al., 2009). A similar scenario may also occur in the mammalian host. Indeed, our demonstration that the N terminus and not the TSR is exposed on salivary gland sporozoites suggests that the initial interaction between sporozoite and liver involves this domain of CSP, a hypothesis which is supported by previous studies demonstrating that the N terminus binds to hepatic HSPGs (Rathore et al., 2001, 2002). However, in contrast to salivary gland invasion, CSP

is cleaved after hepatocyte contact, suggesting that the process of salivary gland invasion is qualitatively different from hepatocyte entry.

In the mammalian host, proteolytic cleavage of CSP regulates the switch to an adhesive conformation, and our data suggest that the highly conserved region I contains the cleavage site. This hypothesis is supported by our previously published antibody mapping experiments as well as pulse–chase metabolic labeling experiments with sporozoites expressing a hybrid CSP (Coppi et al., 2005), which indicated that neither the repeat region nor the upstream portion of the N terminus contain the cleavage site. We have tried to determine the precise cleavage site within region I by N-terminal sequencing of native cleaved CSP; however, this work has never yielded robust reproducible results because of the small amount of native CSP that we are able to isolate from sporozoites. Thus, it remains possible that region I is required for efficient cleavage but does not itself contain the cleavage site. We hypothesize that the small amount of cleavage observed in region I deletion mutants is likely caused by inefficient processing at an alternative, upstream site, although we have not been able to map the alternate cleavage site because of limitations in sporozoite material for these experiments. Overall, the conservation of region I in CSPs from all species of *Plasmodium* in addition to the low infectivity of region I deletion mutants suggest that cleavage is an essential process for sporozoite infectivity.

In contrast to our findings, a previous study in which region I of CSP was deleted found no effect on sporozoite infectivity compared with the parental line (Tewari et al., 2002). However, in that study, the deletion was introduced into a *P. berghei* line in which the endogenous *CSP* gene was replaced by *Plasmodium falciparum CSP*, Pb(PfCSP). Yet this parental line, Pb(PfCSP), invades salivary glands with a 10-fold lower efficiency compared with WT sporozoites (Fig. S8 A; Tewari et al., 2002), raising the possibility that *P. falciparum* CSP does not fold properly on the surface of *P. berghei* sporozoites. To test this, we performed IFAs with Pb(PfCSP) sporozoites and polyclonal antisera specific for the TSR of *P. falciparum* CSP and found that in contrast to WT *P. falciparum* sporozoites, the TSR is accessible to antibodies on the surface of Pb(PfCSP) sporozoites (Fig. S8 C). The exposure of the TSR in the full-length CSP expressed by these parasites begins to explain why deletion of region I does not affect their infectivity for hepatocytes, as cleavage would no longer be necessary for TSR exposure. Furthermore, when we investigated whether these transgenic sporozoites have a lower infectivity for salivary glands as the result of premature exposure of the TSR, we found that this was indeed the case (Fig. S8 B). Together, these data suggest that although the overall structure of CSP is conserved among all *Plasmodium* species, CSPs may not fold correctly in heterologous species.

Our findings are relevant to malaria vaccine development. Sterile immunity to the preerythrocytic stages of *Plasmodium* can be generated with high doses of irradiated sporozoites (Hoffman et al., 2002), and CSP is an important component of this protective response (Kumar et al., 2006).

Indeed, CSP-based subunit vaccines have been a focus of the malaria vaccine effort, culminating in ongoing phase III trials with RTS,S, a vaccine candidate composed of the CSP repeat region and C terminus (Ballou, 2009). RTS,S is designed to include important T cell epitopes from the C terminus that induce cellular responses targeting the infected hepatocyte and B cell epitopes in the repeat region that lead to the production of antibodies targeting the sporozoite. The inclusion of the CSP repeat region in RTS,S reflects previous findings that high antibody titers to this immunodominant region can inhibit sporozoite infectivity in rodent models (Sinnis and Nardin, 2002). Nonetheless, it has been difficult to translate these findings to humans in part because of the difficulty in generating sufficiently high antibody titers (Sinnis and Nardin, 2002). Our current findings are relevant to the generation of protective antibody responses using CSP-based vaccines. First, we show that similar to HIV (Zolla-Pazner, 2004), malaria sporozoites expose a critical cell-adhesive motif at the moment of cell invasion and that this "just-in-time" exposure protects sporozoites from the action of antibodies that target the TSR. Therefore, inclusion of the CSP C terminus in a vaccine should focus on the important T cell epitopes found in this portion of the protein and not on generating TSR-specific antibodies. Second, our work demonstrates that proteolytic processing of CSP is critical for sporozoite infectivity in the mammalian host and suggests that antibodies that specifically target this function could be the foundation for a more potent and effective vaccine. In addition, the conservation of the cleavage site among all species of *Plasmodium* may make it possible to target all human-infecting species with one immunogen. In light of our findings, it is encouraging to note that the antibody response to the N terminus of CSP has recently been shown to be associated with protection (Bongfen et al., 2009). Overall, these data provide important structure–function information that should guide further work in designing subunit malaria vaccines.

## MATERIALS AND METHODS

**Generation of mutant *CSP* genes.** Mutant *CSP* genes were generated using a PCR-based approach (Fig. S1 A). In each case, two gene fragments flanking the region to be deleted and including engineered or endogenous restriction sites were amplified and cut to yield fragments that when ligated made a *CSP* mutant containing the desired deletion. For the ΔRI CSP, the amino acids KLKQP were deleted using the following strategy: a 128-bp 5′ fragment from the *CSP* open reading frame was amplified by PCR using forward primer P1 (5′-GTAT CACGTG CTTAACTCTAAG-3′; existing PmlI site underlined) and P2 (5′-GC AATATT ATTACGCTC-TATTTTTTCG-3′; introduced SspI site underlined). For the ΔNfull mutant, the amino acids NKSIQAQRNLNELCYNEGNDNKLYHV-LNSKNGKIYNRNTVNRLLADAPEGKKNEKKNEKIERNNKLKQP, which encompass the entire N terminus excluding the signal sequence, were deleted as follows: a 5′ 722-bp fragment was amplified using forward primer P5 (5′-AAAAAA GGTACC AAATATTATATGC-3′; existing KpnI site underlined) and reverse primer P6 (5′-AGAG CAGCTCG CCATATCCT-GGAAGTAGAG-3′; introduced PvuII site underlined). For all mutants, a 776-bp 3′ *CSP* fragment was amplified using forward primer P3 (5′-GAGC-GTAATAATAAATTGAAACAA AGGCCT CCACCACCAAACCC-3′; introduced StuI site underlined) and reverse primer P4 (5′-GTTTAT TTA-ATTAA AGAATACTAATAC-3′; existing PacI site underlined). Both PCR products were gel purified using the QIAquick gel extraction kit (QIAGEN)

and then digested with the appropriate restriction enzymes and ligated overnight at 14°C using T4 DNA ligase. Because several ligation products were possible, we performed a PCR amplification of the correct ligation product with primers spanning the 873-bp PmlI–PacI fragment for the ΔRI *CSP* mutant and primers spanning the KpnI–PacI fragment for the ΔNfull *CSP* mutant. Mutant *CSP* genes or gene fragments were then cloned into pCR4-TOPO and sequenced to verify that region I or the entire N terminus was deleted and that the repeat region was intact. The *CSP* PmlI–PacI fragment with region I deleted or the *CSP* Kpn-Pac fragment with the N terminus deleted was then cloned into pCSComp (Thathy et al., 2002) replacing WT *CSP*.

**Generation of mutant parasites.** Recombinant *P. berghei* ANKA strain parasites were generated by double homologous recombination in which the native *CSP* locus was replaced by a WT or mutant copy of *CSP* with its control elements and a selection cassette (Fig. S1 B). The transfection plasmid (pCSRep) was built from pCSComp (Thathy, et al., 2002), which has a drug selection cassette consisting of a copy of the human *DHFR* gene flanked by 2.2 kb of 5′ untranslated region (UTR) and 0.55 kb of 3′ UTR of *P. berghei DHFR-TS*, followed by a *CSP* cassette consisting of a WT copy of the *P. berghei CSP* gene flanked by 1.3 kb of *CSP* 5′ UTR and 450 bp of *CSP* 3′ UTR. To generate a targeting construct that would replace the endogenous *CSP* locus, we cloned additional *CSP* 5′ UTR upstream of the selection cassette. This was obtained from p9.5ΔE (Thathy et al., 2002) between the EcoRV and XbaI sites, using forward (5′-GTG CTC-GAG TAATATATGAAAATAATGAATGAGG-3′; introduced XhoI site underlined) and reverse primer (5′-CTC GTCGAC AATAAATTGGTT-TATGAAATTAGC-3′; introduced HincII site underlined). The resulting 730-bp PCR product was cloned into pCR4-TOPO (Invitrogen), and terminal restriction sites were then added for cloning into pCSComp using forward (5′-AAA CTGCAGCTCGAG TAATATATGAAAATA-ATGAATG-3′; introduced PstI site immediately before the existing XhoI site underlined) and reverse primer (5′-AAAA CTGCAG ACAATA-AATTGGTTTATGAAATTAGC-3′; introduced PstI site underlined). The PCR product was cloned, its sequence verified, and then cloned into the PstI site at the 5′ end of the selection cassette in pCSComp. This final construction was called pCSRep and contained WT or mutant *CSP*. WT *P. berghei* ANKA schizonts collected from Wistar rats were electroporated with 5 μg DNA as previously outlined (Janse et al., 2006), injected into mice, and selected with pyrimethamine and cloned by limiting dilution in mice.

**Southern blot and PCR verification of *CSP* mutants.** Integration of the transfected DNA at the correct location was verified for each recombinant clone by PCR and Southern blotting (Fig. S1 C), and the CSP sequence of the resulting clones was verified by sequencing. PCR to verify integration at the *CSP* locus was performed with primers DP1 (5′-AATGAGAC-TATCCCTAAGGG-3′) and DP2 (5′-TAATTATATGTTATTTTATT-TCCAC-3′). Southern blotting was performed with genomic DNA from erythrocytic stage parasites digested with EcoRV and probed with the 873-bp PmlI–PacI fragment of *CSP*, which was labeled with digoxigenin–dUTP by random priming and detected using the DIG High Prime DNA Labeling and Detection kit (Roche). In addition, the *CSP* coding sequence of each clone was amplified using primers P3 (5′-GAGCTATGTTACAAT-GAAGG-3′) and P4 (5′-AAATTCTAGTATTTTTTCCGCGC-3′) and sequenced to confirm that the deletion was not corrected.

**Mosquito infection.** *Anopheles stephensi* mosquitoes were fed on mice infected with *P. berghei* ANKA RCon or mutant parasites. Days 10–22 after infective blood meal, mosquito midguts, salivary glands, and hemolymph were harvested for determination of sporozoite numbers. For midgut and salivary gland sporozoites, organs from 20 mosquitoes were pooled and homogenized, and released sporozoites were counted using a hemocytometer. Hemolymph from 20 mosquitoes was collected by perfusion of the thorax and abdomen with DME, and sporozoites were counted on a hemocytometer.

**Cells and antibodies.** Hepa1-6 (CRL-1830; American Type Culture Collection) and MDFs (Coppi et al., 2007) were maintained in DME supplemented with 10% FCS and 1 mM glutamine (DME/FCS). HBMVEC, a human endothelial cell line (CC-2811; Cambrex), was grown in EGM-2MV media (Cambrex) supplemented with 5% FCS. mAb 3D11 is directed against the repeat region of *P. berghei* CSP (Yoshida et al.,1980); mAb 2E6 is directed against *Plasmodium* Hsp70 (Tsuji et al., 1994); and UIS-4 antisera, a gift from S. Kappe (Seattle Biomedical Research Institute, Seattle, WA), is specific for the hepatic stage PV (Tarun et al., 2007). Polyclonal antisera to the N- and C-terminal portions of *P. berghei* CSP were generated using peptides that spanned the entire N and C termini of *P. berghei* CSP as previously outlined (Coppi et al., 2005). For experiments testing the effect of α-C serum on hepatocyte invasion, the IgG fraction was isolated by protein A purification (Vivapure maxiprepA; Sartorius).

**Immunoblot of sporozoite lysates.** Sporozoites were lysed in reducing sample buffer, and $10^4$ sporozoite equivalents/lane were loaded and separated by SDS-PAGE and transferred to polyvinylidene fluoride membrane. The membrane was cut between the 52- and 76-kD markers, and the top half was incubated with a 1:100 dilution of rabbit polyclonal antisera to the repeat region of *P. berghei* TRAP followed by anti–rabbit Ig conjugated to horseradish peroxidase, and the bottom half was incubated with 1 μg/ml mAb 3D11 followed by anti–mouse Ig conjugated to horseradish peroxidase. Bound antibodies were visualized using enhanced chemiluminescence (GE Healthcare).

**Metabolic labeling and immunoprecipitation.** *P. berghei* sporozoites were metabolically labeled in DME without Cys/Met, 1% BSA, and 400 μCi/ml L-[$^{35}$S]Cys/Met for 1 h at 28°C and then kept on ice or chased at 28°C for the indicated times as outlined previously (Coppi et al., 2005). To investigate the kinetics of processing in the presence of hepatocytes, sporozoites were labeled as above, chased at 28°C for 1 h, and then centrifuged (300 *g*) onto Hepa1-6 cells on glass coverslips and subjected to an additional chase for 5, 15, or 30 min at 37°C. In all cases, chased sporozoites were lysed, and labeled CSP was immunoprecipitated with mAb 3D11 conjugated to Sepharose, eluted from the beads, and analyzed by SDS-PAGE using 10 × 10.5–cm gels (SE260 system; Hoefer) followed by autoradiography.

**Immunofluorescence.** Sporozoites from oocysts, hemolymph, and salivary glands were fixed with 4% PFA, washed, blocked with PBS/BSA, and incubated with polyclonal α-N or α-C sera (1:100 dilution), followed by anti–rabbit Ig-FITC or 1 μg/ml mAb 3D11, followed by anti–mouse Ig. The total number of sporozoites was counted by phase-contrast microscopy, and the percentage of sporozoite staining was determined by fluorescence microscopy. For cell contact experiments, sporozoites were centrifuged onto coverslips with Hepa1-6 cells at 4°C and then incubated at 37°C for the indicated time points, fixed with 4% PFA, and stained with α-N or α-C sera for 75 min. For these experiments, we visualized all sporozoites with 0.05 μg/ml mAb 3D11 added during the last 15 min of incubation. Binding of antibodies was revealed with anti–rabbit Alexa Fluor 594 and anti–mouse Ig-FITC. Specimens were photographed using a fluorescence microscope (E600; Nikon) and a digital camera (DXM1200; Nikon).

**Electron microscopy.** Midguts from infected mosquitoes were dissected at days 8, 10, and 12 after blood meal, fixed in 1% glutaraldehyde and 4% PFA in PBS for 5 d, and postfixed in 1% osmium tetroxide and 1.5% $K_3Fe(CN)_6$ in PBS for 2 h, followed by incubation in 0.5% uranyl acetate for 1 h. Midguts were dehydrated in increasing concentrations of ethanol and then incubated for 1 h in propylene oxide, followed by another incubation for 1 h in a 1:1 mixture of propylene oxide and Epon (Electron Microscopy Sciences). Specimens were subsequently embedded in Epon at 60°C for 2 d. Photographs were taken with a transmission electron microscope (EM10; Carl Zeiss, Inc.).

**Invasion and development assays.** 5 × $10^4$ sporozoites were added to Hepa1-6, MDFs, or HBMVEC cells in Lab-Tek wells. In some experiments, sporozoites were preincubated with 10 μM E-64d for 15 min at 25°C to determine the proportion of intracellular sporozoites that had productively invaded. For experiments testing the effect of α-C serum on invasion, sporozoites were added to the cells in the presence of a 1:10 dilution of the antiserum. For all invasion assays, sporozoites were incubated with cells for 1 h at 37°C, washed, fixed, and stained with a double staining assay that distinguishes intracellular from extracellular sporozoites (Rénia et al.,1988). To assess productive invasion by ΔNfull sporozoites, sporozoites were incubated with cells for 6 h at 37°C, washed, fixed with methanol, and stained with UIS-4 antiserum (1:500 dilution), followed by anti–rabbit Ig–Alexa Fluor 594 and 1 μg/ml mAb 3D11, followed by anti–mouse Ig-FITC. To quantify EEF development, cells with sporozoites were grown for an additional 2 d, after which they were fixed with methanol and stained with mAb 2E6, followed by anti–mouse Ig-FITC.

**Quantification of liver stage burden.** Swiss Webster and C57BL/6 mice were injected i.v. or i.d. with $10^4$ sporozoites. 40 h later, livers were harvested, total RNA was isolated, and liver parasite burden was quantified by RT-qPCR as outlined previously (Bruña-Romero et al., 2001) using primers that recognize *P. berghei*–specific sequences within the 18S rRNA (Kumar et al., 2004). 10-fold dilutions of a plasmid construct containing the *P. berghei* 18S rRNA gene were used to create a standard curve. For experiments testing the effect of α-C serum on hepatocyte invasion, mice were injected i.v. with 1.5 mg of Ig fraction and 5 min later injected i.v. with sporozoites.

**Determination of prepatent period.** Mice were injected i.v. or i.d. with the indicated number of sporozoites, and the onset of blood stage infection was determined by observation of Giemsa-stained blood smears, beginning on day 3 after inoculation.

**Quantification of sporozoites in mosquito organs.** Midguts, salivary glands, thoraces, and abdomens from 20 infected mosquitoes were dissected, added to 1 ml of Tri-Reagent containing 5 μl polyacryl carrier, and homogenized, and total RNA was isolated. The number of sporozoites in each sample was determined by RT-qPCR using primers that recognize *P. berghei*–specific sequences within the 18S rRNA as outlined previously (Bruña-Romero et al., 2001; Kumar et al., 2004). Sporozoite numbers were determined using a standard curve of $10^2$ to $10^5$ sporozoites that were processed in the same way the samples were processed.

**Quantification of parasite number in the skin.** The number of parasites remaining in the inoculation site was determined as previously described (Yamauchi et al., 2007). In brief, Swiss Webster mice were anesthetized, and 5,000 sporozoites were injected i.d. into the pinna of the ear. The injected ears were removed at the indicated time points, weighed, cut into small pieces, and digested overnight at 50°C with proteinase K. Total genomic DNA was extracted using the DNeasy tissue kit (QIAGEN), and parasite DNA was quantified using nested PCR followed by qPCR as previously outlined (Yamauchi et al., 2007). Parasite numbers were determined using a standard curve made from mouse ears spiked with 0, 200, 1,000, and 5,000 sporozoites that were processed in the same way the experimental samples were processed.

**Quantification of gene expression in skin parasites.** Swiss Webster mice were anesthetized, and 5,000 sporozoites in 5 μl were injected i.d. into the pinna of the ear. RNA extraction and RT-qPCR were performed as previously outlined (Medica and Sinnis, 2005). At the indicated time points, the injected ears were removed, weighed, snap frozen in liquid nitrogen, and stored at −80°C until RNA was extracted. The weight of each excised ear did not exceed 20 mg. Ears were then homogenized in 1.6 ml of Tri-Reagent using a Brinkmann Polytron homogenizer for 1 min and extracted with 320 μl chloroform. The aqueous phase was removed and mixed with an equal volume of 70% ethanol, and RNA was isolated using an RNeasy Mini spin column (QIAGEN) according to the manufacturer's instructions.

Total RNA was eluted with 40 µl water, and RT-qPCR was performed with 1/20th of the total volume using the one-step QuantiTect SYBR Green RT-PCR kit (QIAGEN). The temperature profile was as follows: 50°C for 30 min and 95°C for 15 min, followed by 40 cycles of 95°C for 30 s, 43°C for 30 s, 72°C for 30 s, and 76.3°C for 15 s, the final step being for data acquisition. Primers that recognize *P. berghei* TLP (Moreira et al., 2008) and MSP-1 (forward primer, 5′-GCAATTTATCAACTTCATCCTGT-3′; reverse primer, 5′-CATTTGTAGCTAAATCTTCTGTT-3′) were used. 10-fold dilutions of a plasmid containing either the TLP or MSP-1 fragment were used to create a standard curve.

**Statistics.** Data are presented as mean ± SD. Statistics were generated using the unpaired Student's *t* test, and p-values <0.01 were considered significant. All experiments using animals were approved by Institutional Animal Care and Use Committee at the New York University School of Medicine.

**Online supplemental material.** Fig. S1 shows construction and verification of *CSP* mutant parasites. Fig. S2 shows oocyst numbers in *CSP* mutant parasites. Fig. S3 shows EEF size of *CSP* mutant parasites. Fig. S4 shows gliding motility and cell traversal of *CSP* mutant parasites. Fig. S5 shows fine specificity of C-terminal antiserum. Fig. S6 shows surface staining of oocyst and salivary gland sporozoites of ΔRI mutants. Fig. S7 shows electron microscopy images of ΔNfull mutant oocysts. Fig. S8 shows mosquito distribution and immunofluorescence experiments of Pb(PfCSP) sporozoites. Table S1 lists sporozoite numbers in mosquitoes infected with *CSP* mutants. Table S2 shows localization of salivary gland sporozoites in *CSP* mutants. Online supplemental material is available at http://www.jem .org/cgi/content/full/jem.20101488/DC1.

## REFERENCES

Adams, J.C., and R.P. Tucker. 2000. The thrombospondin type 1 repeat (TSR) superfamily: diverse proteins with related roles in neuronal development. *Dev. Dyn.* 218:280–299. doi:10.1002/(SICI)1097-0177(200006)218:2<280::AID-DVDY4>3.0.CO;2-0

Aley, S.B., M.D. Bates, J.P. Tam, and M.R. Hollingdale. 1986. Synthetic peptides from the circumsporozoite proteins of *Plasmodium falciparum* and *Plasmodium knowlesi* recognize the human hepatoma cell line HepG2-A16 in vitro. *J. Exp. Med.* 164:1915–1922. doi:10.1084/jem.164.6.1915

Amino, R., S. Thiberge, B. Martin, S. Celli, S. Shorte, F. Frischknecht, and R. Ménard. 2006. Quantitative imaging of *Plasmodium* transmission from mosquito to mammal. *Nat. Med.* 12:220–224. doi:10.1038/nm1350

Amino, R., D. Giovannini, S. Thiberge, P. Gueirard, B. Boisson, J.F. Dubremetz, M.C. Prévost, T. Ishino, M. Yuda, and R. Ménard. 2008. Host cell traversal is important for progression of the malaria parasite through the dermis to the liver. *Cell Host Microbe.* 3:88–96. doi:10.1016/j.chom.2007.12.007

Ballou, W.R. 2009. The development of the RTS,S malaria vaccine candidate: challenges and lessons. *Parasite Immunol.* 31:492–500. doi:10.1111/j.1365-3024.2009.01143.x

Bongfen, S.E., P.M. Ntsama, S. Offner, T. Smith, I. Felger, M. Tanner, P. Alonso, I. Nebie, J.F. Romero, O. Silvie, et al. 2009. The N-terminal domain of *Plasmodium falciparum* circumsporozoite protein represents a target of protective immunity. *Vaccine.* 27:328–335.

Bruña-Romero, O., J.C. Hafalla, G. González-Aseguinolaza, G. Sano, M. Tsuji, and F. Zavala. 2001. Detection of malaria liver-stages in mice infected through the bite of a single *Anopheles* mosquito using a highly sensitive real-time PCR. *Int. J. Parasitol.* 31:1499–1502. doi:10.1016/S0020-7519(01)00265-X

Cerami, C., U. Frevert, P. Sinnis, B. Takacs, P. Clavijo, M.J. Santos, and V. Nussenzweig. 1992. The basolateral domain of the hepatocyte plasma membrane bears receptors for the circumsporozoite protein of *Plasmodium falciparum* sporozoites. *Cell.* 70:1021–1033. doi:10.1016/0092-8674(92)90251-7

Cerami, C., U. Frevert, P. Sinnis, B. Takacs, and V. Nussenzweig. 1994. Rapid clearance of malaria circumsporozoite protein (CS) by hepatocytes. *J. Exp. Med.* 179:695–701. doi:10.1084/jem.179.2.695

Chatterjee, S., M. Wery, P. Sharma, and V.S. Chauhan. 1995. A conserved peptide sequence of the *Plasmodium falciparum* circumsporozoite protein and antipeptide antibodies inhibit *Plasmodium berghei* sporozoite invasion of Hep-G2 cells and protect immunized mice against *P. berghei* sporozoite challenge. *Infect. Immun.* 63:4375–4381.

Coppi, A., C. Pinzon-Ortiz, C. Hutter, and P. Sinnis. 2005. The *Plasmodium* circumsporozoite protein is proteolytically processed during cell invasion. *J. Exp. Med.* 201:27–33. doi:10.1084/jem.20040989

Coppi, A., R. Tewari, J.R. Bishop, B.L. Bennett, R. Lawrence, J.D. Esko, O. Billker, and P. Sinnis. 2007. Heparan sulfate proteoglycans provide a signal to *Plasmodium* sporozoites to stop migrating and productively invade host cells. *Cell Host Microbe.* 2:316–327. doi:10.1016/j.chom.2007.10.002

Frevert, U., P. Sinnis, C. Cerami, W. Shreffler, B. Takacs, and V. Nussenzweig. 1993. Malaria circumsporozoite protein binds to heparan sulfate proteoglycans associated with the surface membrane of hepatocytes. *J. Exp. Med.* 177:1287–1298. doi:10.1084/jem.177.5.1287

Gantt, S.M., J.M. Myung, M.R.S. Briones, W.D. Li, E.J. Corey, S. Omura, V. Nussenzweig, and P. Sinnis. 1998. Proteasome inhibitors block development of *Plasmodium* spp. *Antimicrob. Agents Chemother.* 42:2731–2738.

Ghosh, A.K., M. Devenport, D. Jethwaney, D.E. Kalume, A. Pandey, V.E. Anderson, A.A. Sultan, N. Kumar, and M. Jacobs-Lorena. 2009. Malaria parasite invasion of the mosquito salivary gland requires interaction between the *Plasmodium* TRAP and the *Anopheles* saglin proteins. *PLoS Pathog.* 5:e1000265. doi:10.1371/journal.ppat.1000265

Greenwood, B.M., K. Bojang, C.J. Whitty, and G.A. Targett. 2005. Malaria. *Lancet.* 365:1487–1498. doi:10.1016/S0140-6736(05)66420-3

Gueirard, P., J. Tavares, S. Thiberge, F. Bernex, T. Ishino, G. Milon, B. Franke-Fayard, C.J. Janse, R. Ménard, and R. Amino. 2010. Development of the malaria parasite in the skin of the mammalian host. *Proc. Natl. Acad. Sci. USA.* 107:18640–18645. doi:10.1073/pnas.1009346107

Hoffman, S.L., L.M.L. Goh, T.C. Luke, I. Schneider, T.P. Le, D.L. Doolan, J. Sacci, P. de la Vega, M. Dowler, C. Paul, et al. 2002. Protection of humans against malaria by immunization with radiation-attenuated *Plasmodium falciparum* sporozoites. *J. Infect. Dis.* 185:1155–1164. doi:10.1086/339409

Janse, C.J., B. Franke-Fayard, G.R. Mair, J. Ramesar, C. Thiel, S. Engelmann, K. Matuschewski, G.J. van Gemert, R.W. Sauerwein, and A.P. Waters. 2006. High efficiency transfection of *Plasmodium berghei* facilitates novel selection procedures. *Mol. Biochem. Parasitol.* 145:60–70. doi:10.1016/j.molbiopara.2005.09.007

Kariu, T., M. Yuda, K. Yano, and Y. Chinzei. 2002. MAEBL is essential for malarial sporozoite infection of the mosquito salivary gland. *J. Exp. Med.* 195:1317–1323. doi:10.1084/jem.20011876

Kumar, K.A., G.A. Oliveira, R. Edelman, E. Nardin, and V. Nussenzweig. 2004. Quantitative *Plasmodium* sporozoite neutralization assay (TSNA). *J. Immunol. Methods.* 292:157–164. doi:10.1016/j.jim.2004.06.017

Kumar, K.A., G. Sano, S. Boscardin, R.S. Nussenzweig, M.C. Nussenzweig, F. Zavala, and V. Nussenzweig. 2006. The circumsporozoite protein is an immunodominant protective antigen in irradiated sporozoites. *Nature.* 444:937–940. doi:10.1038/nature05361

Medica, D.L., and P. Sinnis. 2005. Quantitative dynamics of *Plasmodium yoelii* sporozoite transmission by infected anopheline mosquitoes. *Infect. Immun.* 73:4363–4369. doi:10.1128/IAI.73.7.4363-4369.2005

Ménard, R. 2000. The journey of the malaria sporozoite through its hosts: two parasite proteins lead the way. *Microbes Infect.* 2:633–642. doi:10.1016/S1286-4579(00)00362-2

Ménard, R., A.A. Sultan, C. Cortes, R. Altszuler, M.R. van Dijk, C.J. Janse, A.P. Waters, R.S. Nussenzweig, and V. Nussenzweig. 1997. Circumsporozoite protein is required for development of malaria sporozoites in mosquitoes. *Nature.* 385:336–340. doi:10.1038/385336a0

Moreira, C.K., T.J. Templeton, C. Lavazec, R.E. Hayward, C.V. Hobbs, H. Kroeze, C.J. Janse, A.P. Waters, P. Sinnis, and A. Coppi. 2008. The *Plasmodium* TRAP/MIC2 family member, TRAP-Like Protein (TLP), is involved in tissue traversal by sporozoites. *Cell. Microbiol.* 10:1505–1516. doi:10.1111/j.1462-5822.2008.01143.x

Mota, M.M., G. Pradel, J.P. Vanderberg, J.C.R. Hafalla, U. Frevert, R.S. Nussenzweig, V. Nussenzweig, and A. Rodríguez. 2001. Migration of *Plasmodium* sporozoites through cells before infection. *Science.* 291:141–144. doi:10.1126/science.291.5501.141

Mota, M.M., J.C.R. Hafalla, and A. Rodriguez. 2002. Migration through host cells activates *Plasmodium* sporozoites for infection. *Nat. Med.* 8:1318–1322. doi:10.1038/nm785

Myung, J.M., P. Marshall, and P. Sinnis. 2004. The *Plasmodium* circumsporozoite protein is involved in mosquito salivary gland invasion by sporozoites. *Mol. Biochem. Parasitol.* 133:53–59. doi:10.1016/j.molbiopara.2003.09.002

Pinzon-Ortiz, C., J. Friedman, J. Esko, and P. Sinnis. 2001. The binding of the circumsporozoite protein to cell surface heparan sulfate proteoglycans is required for *plasmodium* sporozoite attachment to target cells. *J. Biol. Chem.* 276:26784–26791. doi:10.1074/jbc.M104038200

Pradel, G., S. Garapaty, and U. Frevert. 2002. Proteoglycans mediate malaria sporozoite targeting to the liver. *Mol. Microbiol.* 45:637–651. doi:10.1046/j.1365-2958.2002.03057.x

Rathore, D., T.F. McCutchan, D.N. Garboczi, T. Toida, M.J. Hernáiz, L.A. LeBrun, S.C. Lang, and R.J. Linhardt. 2001. Direct measurement of the interactions of glycosaminoglycans and a heparin decasaccharide with the malaria circumsporozoite protein. *Biochemistry.* 40:11518–11524. doi:10.1021/bi0105476

Rathore, D., J.B. Sacci, P. de la Vega, and T.F. McCutchan. 2002. Binding and invasion of liver cells by *Plasmodium falciparum* sporozoites. Essential involvement of the amino terminus of circumsporozoite protein. *J. Biol. Chem.* 277:7092–7098. doi:10.1074/jbc.M106862200

Rénia, L., F. Miltgen, Y. Charoenvit, T. Ponnudurai, J.P. Verhave, W.E. Collins, and D. Mazier. 1988. Malaria sporozoite penetration. A new approach by double staining. *J. Immunol. Methods.* 112:201–205. doi:10.1016/0022-1759(88)90358-4

Saenz, F.E., B. Balu, J. Smith, S.R. Mendonca, and J.H. Adams. 2008. The transmembrane isoform of *Plasmodium* falciparum MAEBL is essential for the invasion of *Anopheles* salivary glands. *PLoS One.* 3:e2287. doi:10.1371/journal.pone.0002287

Sidjanski, S., and J.P. Vanderberg. 1997. Delayed migration of *Plasmodium* sporozoites from the mosquito bite site to the blood. *Am. J. Trop. Med. Hyg.* 57:426–429.

Sidjanski, S.P., J.P. Vanderberg, and P. Sinnis. 1997. *Anopheles stephensi* salivary glands bear receptors for region I of the circumsporozoite protein of *Plasmodium falciparum*. *Mol. Biochem. Parasitol.* 90:33–41. doi:10.1016/S0166-6851(97)00124-2

Sinden, R.E., and K. Strong. 1978. An ultrastructural study of the sporogonic development of *Plasmodium falciparum* in *Anopheles gambiae*. *Trans. R. Soc. Trop. Med. Hyg.* 72:477–491. doi:10.1016/0035-9203(78)90167-0

Sinden, R.E., A. Suhrbier, C.S. Davies, S.L. Fleck, K. Hodivala, and J.C. Nicholas. 1990. The development and routine application of high-density exoerythrocytic-stage cultures of *Plasmodium berghei*. *Bull. World Health Organ.* 68:115–125.

Sinnis, P., and E. Nardin. 2002. Sporozoite antigens: biology and immunology of the circumsporozoite protein and thrombospondin related anonymous protein. *In* Malaria Immunology. P. Perlmann and M. Troye-Blomberg, editors. S. Karger AG, Basel, Switzerland. 70–96.

Sinnis, P., P. Clavijo, D. Fenyö, B.T. Chait, C. Cerami, and V. Nussenzweig. 1994. Structural and functional properties of region II-plus of the malaria circumsporozoite protein. *J. Exp. Med.* 180:297–306. doi:10.1084/jem.180.1.297

Sinnis, P., T.E. Willnow, M.R.S. Briones, J. Herz, and V. Nussenzweig. 1996. Remnant lipoproteins inhibit malaria sporozoite invasion of hepatocytes. *J. Exp. Med.* 184:945–954. doi:10.1084/jem.184.3.945

Springer, T.A. 1990. Adhesion receptors of the immune system. *Nature.* 346:425–434. doi:10.1038/346425a0

Suarez, J.E., M. Urquiza, A. Puentes, J.E. Garcia, H. Curtidor, M. Ocampo, R. Lopez, L.E. Rodriguez, R. Vera, M. Cubillos, et al. 2001. *Plasmodium falciparum* circumsporozoite (CS) protein peptides specifically bind to HepG2 cells. *Vaccine.* 19:4487–4495. doi:10.1016/S0264-410X(01)00203-1

Tarun, A.S., R.F. Dumpit, N. Camargo, M. Labaied, P. Liu, A. Takagi, R. Wang, and S.H. Kappe. 2007. Protracted sterile protection with *Plasmodium yoelii* pre-erythrocytic genetically attenuated parasite malaria vaccines is independent of significant liver-stage persistence and is mediated by CD8+ T cells. *J. Infect. Dis.* 196:608–616. doi:10.1086/519742

Tewari, R., R. Spaccapelo, F. Bistoni, A.A. Holder, and A. Crisanti. 2002. Function of region I and II adhesive motifs of *Plasmodium falciparum* circumsporozoite protein in sporozoite motility and infectivity. *J. Biol. Chem.* 277:47613–47618. doi:10.1074/jbc.M208453200

Tewari, R., D. Rathore, and A. Crisanti. 2005. Motility and infectivity of *Plasmodium berghei* sporozoites expressing avian *Plasmodium gallinaceum* circumsporozoite protein. *Cell. Microbiol.* 7:699–707. doi:10.1111/j.1462-5822.2005.00503.x

Thathy, V., H. Fujioka, S. Gantt, R. Nussenzweig, V. Nussenzweig, and R. Ménard. 2002. Levels of circumsporozoite protein in the *Plasmodium* oocyst determine sporozoite morphology. *EMBO J.* 21:1586–1596. doi:10.1093/emboj/21.7.1586

Tsuji, M., D. Mattei, R.S. Nussenzweig, D. Eichinger, and F. Zavala. 1994. Demonstration of heat-shock protein 70 in the sporozoite stage of malaria parasites. *Parasitol. Res.* 80:16–21. doi:10.1007/BF00932618

Yamauchi, L.M., A. Coppi, G. Snounou, and P. Sinnis. 2007. *Plasmodium* sporozoites trickle out of the injection site. *Cell. Microbiol.* 9:1215–1222. doi:10.1111/j.1462-5822.2006.00861.x

Yoshida, N., R.S. Nussenzweig, P. Potocnjak, V. Nussenzweig, and M. Aikawa. 1980. Hybridoma produces protective antibodies directed against the sporozoite stage of malaria parasite. *Science.* 207:71–73. doi:10.1126/science.6985745

Zolla-Pazner, S. 2004. Identifying epitopes of HIV-1 that induce protective antibodies. *Nat. Rev. Immunol.* 4:199–210. doi:10.1038/nri1307